2026 IEEE International Conference on Robotics and Automation (ICRA 2026)
June 1-5, 2026. Vienna, Austria

APEX-Glove: An Actuated, Open-Source, Hand-Exoskeleton Glove for Finger Motion Tracking and Kinesthetic 3D Force Feedback

Nicolas Kosanovic[1*] and Jean Chagas Vaz[2]

***Abstract*— Accurate motion tracking and haptics are pivotal to building platforms for immersive Virtual Reality, dexterous robotic hand teleoperation, or embodied AI data collection. Existing technologies fail to provide accurate finger motion tracking *and* multidimensional force feedback simultaneously, complicating robotic hand control. This work develops the APEX-Glove: the world's first dorsal-mounted *wearable* hand exoskeleton yielding both accurate finger motion tracking and active kinesthetic 3D force feedback. Data-driven modeling of the exoskeleton and its Dynamixel XL330 actuators compensates gravity, Coriolis, and friction forces to improve transparency and comfort. Biomechanically-informed analytical inverse kinematics estimates human finger joint angles at 300 Hz with an average Root Mean Squared Error of 18.5° when compared to industrial-grade datagloves (MANUS Quantum Metagloves). Stationary testing finds that the APEX-Glove can generate up to 0.8 N, 0.7 N, and 1.4 N of force feedback in the x, y, and z directions, on average. Motion retargeting to humanoid robot hands is also detailed, with hardware experimentation demonstrating haptic hand teleoperation. Lastly, we open-source[3] the APEX-Glove's cost-effective ($< 700\ USD$) design to disseminate its motion capture and force feedback capabilities to the community.**

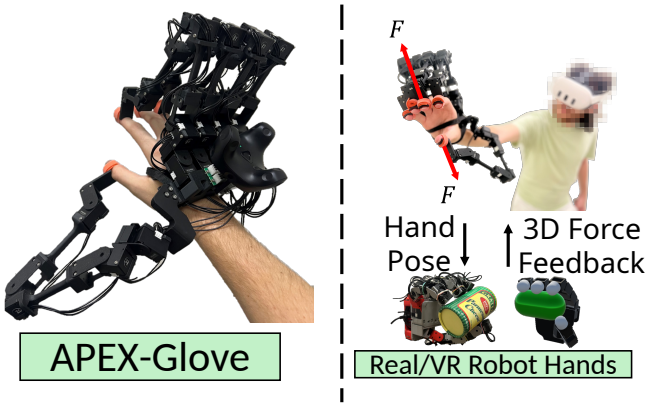

Fig. 1: The APEX-Glove (left) enables a user to teleoperate humanoid hands and feel 3D force feedback on all fingers.

I. INTRODUCTION

Intelligent object manipulation inherently demands precise movement, tactile sensing, and force control to tackle complex tasks. That being said, many cutting-edge Virtual Reality (VR) and robot teleoperation systems used to demonstrate new behaviors to AI models *lack* operator-side force feedback capabilities [1]–[3]. Thus, users cannot complete tasks with certainty using their physical intuition; they must instead *guess* the interaction forces they apply to their environment. While the robot agents themselves may have sensors to measure contact forces, a user without a haptic display cannot rely on kinesthetic information for control, resulting in awkward/unnatural behavior. This is particularly problematic for contact-rich manipulation, which such systems typically struggle with. Moreover, because many AI models are trained on teleoperation data [4], tactile unawareness is passed on from human demonstrators to autonomous machines, resulting in poor autonomous performance. Multiple studies have found that enhancing operator force awareness via kinesthetic teaching [5]–[8], bilateral control [9]–[12], or wearable haptic devices [13]–[16] verifiably result in more capable teleoperation systems *and* autonomous policies, especially with regards to contact-rich tasks. Similar developments have not yet been made for haptic teleoperation of humanoid robot hands.

Humanoid hand teleoperation is commonly realized using data gloves and an egocentric vision system [1]. Supplying users with purely visual feedback complicates general operations, especially when hand geometry causes visual occlusions during grasping. Thus, [13], [15], [16] integrated haptic gloves/exoskeletons into robot avatars to provide users with some tactile feedback (vibrations, cutaneous skin deformation, and flexion resistance) when touching objects. Despite these operational improvements, existing hand-wearable haptic devices do not provide appropriate multidimensional finger-scale force feedback and motion capture for complex robotic hand control. Many such devices only generate passive, unidirectional 1D finger-scale forces to restrict hand closure [18], [19]. Thus, tangible interactions in the axial and abductional directions cannot be rendered, limiting an operator's tactile perception. Moreover, the finger pose estimation provided by haptic gloves is often inferior to that of pure motion capture systems. From [5]–[8], [17], [20], **force feedback and finger tracking are the primary bottlenecks preventing teleoperated robotic hands from complex in-hand manipulation**. Hence, wearable haptic devices need to be improved to enable advanced teleoperation control for humanoid robot hands.

[1*]N. Kosanovic is a PhD student with the Department of Electrical and Computer Engineering, University of Louisville. *direct all correspondence to this author. nicolas.kosanovic@louisville.edu

[2]Dr. Jean Chagas Vaz is with the Faculty of Electrical and Computer Engineering, University of Louisville, Louisville, KY, 40208, USA. jean.chagasvaz@louisville.edu

[3]https://nicks-robots.com/apex-glove/.

Literature Review

From the 1990 *CyberGrasp* [21] to the 2025 *DOGlove* [22], many wearable haptic gloves for robot hand control have been proposed. Nearly all of these devices feature exclusively unidirectional force feedback [18], [19], [23]–[25]. This is commonly attributed to limitations in actuation technology; inexpensive, small, lightweight, and torque-controlled smart servos were not commercially available until recently. Physical constraints on motor size and its relation to output torques [26] required compact servo manufacturers to use higher reduction ratios to compensate. This disproportionally affects backdrivability and apparent inertia, which scale with the square of the gear ratio [27]. These characteristics complicate force control, especially within haptic applications. As such, traditional approaches for generating 3D force feedback, like kinesthetic coupling with externally-grounded robot arms [27], could not be feasibly miniaturized into a hand-wearable package.

Thus, [19], [21], [24], [25] used high-force tendon drives on exoskeletons to produce resistive fingertip-scale feedback instead. While inexpensive, lightweight, and powerful, such tendon drives can only produce unidirectional forces. Actuated exoskeletons [18], [22], [23] produce weaker, yet bidirectional 1D forces using driven mechanical linkages instead. Straying from *wearable exoskeletons*, two systems capable of producing fingertip-level 3D force feedback were developed by [28], [29]. Both consist of externally-grounded robotic arms with multifingered, force-controlled hands whose distal links connect to user fingertips via magnetic couplers. These systems display forces *kinesthetically* via the movement of these manipulators. Additionally, these setups introduce coupled arm-scale feedback via externally-grounded robotic arms. Despite their advanced capabilities, such systems are significantly more expensive, immobile, and human workspace-restrictive than the aforementioned wearable exoskeletons, further complicating general adoption.

Beyond feedback, human-machine interfaces for teleoperation commonly provide motion capture, specifically hand pose estimation. Exoskeletons are particularly powerful in this regard, as forward kinematics immediately obtains human fingertip pose information. For dorsally-mounted exoskeletons, human finger joint angles can be obtained analytically through geometric inverse kinematics, given calibration to determine a user's knuckle positions [20], [23], [30]. Contrarily, the palm-facing externally-grounded systems from [28], [29] cannot deterministically locate user hand pose, yielding a floating-base inverse kinematics problem that can be solved via additional external trackers. Alternatively, [21], [24], [25] use magnetic pose sensing, tendon draw length, and flex sensors to infer hand pose, with the latter two attaining worse tracking accuracy than magnetic/exoskeletal systems [31].

To reiterate: **no existing wearable hand exoskeleton is capable of producing 3D force feedback**. The lack of such capabilities has been a major bottleneck highlighted within telepresence and robotic learning [17]. In this paper, we address this critical gap in wearable exoskeletal haptics by developing the APEX-Glove: an Actuated, Open-Source Hand-Exoskeleton Glove for finger motion tracking and fingertip 3D force feedback (Figure 1, left). With the advent of small, lightweight, low-cost, torque-controlled smart servos (ROBOTIS Dynamixel XL330), it is possible to render multidimensional forces kinesthetically via small manipulators [9], [10]. Data-driven modeling is used to compensate for dynamical effects, friction, and gravity, enhancing transparency and comfort over [20]. Furthermore, the inexpensive (sub-700 USD) APEX-Glove uses human finger biomechanics to analytically determine a user's finger joint angles. Hand pose estimation accuracy is compared to the 5000 USD MANUS Quantum Metagloves, an industrial-grade hand motion capture device. After that, human motion retargeting to several popular robotic hands is demonstrated in simulation and on real hardware. Lastly, the APEX-Glove's hardware, software, and assembly are open-sourced to disseminate the motion capture and 3D force feedback capabilities of this device to the broader community.

Paper Contributions

1) The design, development, and evaluation of a wearable hand exoskeleton with 3D force feedback, finger motion tracking, and dynamic compensation.
2) Data-driven models and software to enable transparent torque control on low-cost Dynamixel actuators.
3) Demonstration of and methods for motion retargeting towards haptic dexterous hand teleoperation.

Article Structure

This article consists of five main sections: Section II details the theory, hardware, and software realization of the APEX-Glove. Section III overviews the experimental campaign, including retargeting human hand motions to simulated/real robotic hands. Section IV analyzes experimental data, discusses the device, and compares it to similar works. Lastly, Section V concludes the article, highlighting the APEX-Glove's strengths and limitations while also describing future improvements.

II. Proposed Methodology

This section details the theory, design, and realization of the APEX-Glove for applications spanning from general VR usage to real robot teleoperation.

A. Theoretical Framework

Haptic exoskeletons for manipulation must be able to estimate a user's hand pose and apply force feedback. The following two subsections tackle these objectives from first principles to motivate the APEX-Glove's design.

1) Hand Pose Estimation: Inferring human finger joint angles with a dorsal-mounted linkage has been well-documented and demonstrates nearly state-of-the-art motion tracking performance when properly calibrated [20], [30]. Human fingers are commonly modeled as RRRR serial

linkages with all but their first axes being parallel, as shown in Figure 2. Given details like the knuckle frame's spatial pose O_{h0}, phalangeal lengths L_{h1}, L_{h2}, L_{h3}, and the fingertip pose O_{h4}, inverse kinematics (IK) computes human finger joint angles. Moreover, the finger's simple structure enables IK to be solved analytically. By moving from the fingertip frame O_{h4} along its $-x_{h4}$ axis by a distance of the distal phalanx length L_{h3}, the DIP joint frame O_{h3} is located. Simultaneously, the MCP adduction joint angle q_{h0} is the corresponding rotation that aligns the finger flexion plane $x_{h0}z_{h0}$ with the DIP joint frame O_{h3}. From here, the proximal and middle phalanges form an intermediate 2-DoF planar RR linkage between the MCP and DIP flexion joints. Solving IK for this intermediate RR linkage is trivial analytically [20] and yields two solutions for MCP and PIP flexion joint angles q_{h1}, q_{h2}. The solution corresponding to an "elbow-up" configuration enforces a biomechanical constraint ($q_{h2} \geq 0°$) and should therefore always be selected. Finally, the planar fingertip pitch relative to the knuckle ϕ is used with q_{h1}, q_{h2} to calculate the DIP flexion joint angle as $q_{h3} = \phi - q_{h1} - q_{h2}$.

With this base technique for hand pose estimation established, constraints/assumptions can be imposed to guide kinematic structure design. For instance, the previous analysis demanded fingertip spatial pose information, which is 6D in Cartesian space (x,y,z,$roll$,$pitch$,yaw). Biomechanically speaking, a DIP joint is incapable of independently rolling or yawing; moreover, the simple kinematic structure can be treated as a planar linkage decoupled from q_{h0}. Thus, if the Cartesian position of the DIP joint frame O_{h3} and pitch ϕ are measured directly, then the kinematics are still solvable, even without prior knowledge of O_{h4}. **As such, a minimum of four DoFs are needed to infer human finger positions**, assuming that the MCP abduction and mechanism yaw joints are approximately collinear. If not, reciprocal wrenches can generate internal stresses in an exoskeleton's structural linkages, as per [30].

The linkage atop the hand in Figure 2 shows a candidate 4 DoF RRRR mechanism for tracking the position of frame O_{h3} and pitch ϕ. In the case where z_0 and z_{h0} are approximately collinear, $q_{h0} = q_0$, and the linkage becomes a planar 6-bar hexagonal linkage, which has 3 DoF. Given exoskeleton joint angles q_1, q_2, and q_3 (corresponding to frames O_1, O_2, and O_3), all other joint positions, namely those of the finger, are fully constrained. Thus, the linkage is fixed relative to the finger, and no kinematic redundancy exists within the system.

The transformation from the exoskeleton base frame O_0 to the knuckle frame O_{h0} is $T_{O_0O_{h0}}$ (black dashed line from Figure 2), which is calibrated via an arc-fitting algorithm [30]. This constitutes repeatedly recording the forward kinematics of the linkage while continuously moving the erected finger. Due to the MCP joint's two degrees of freedom, the forward kinematics will trace a path on a 3D sphere whose center coordinates and radius are the knuckle's Cartesian position and the total length of the finger L_h. If the finger is assumed to have average human proportions, L_{h1},

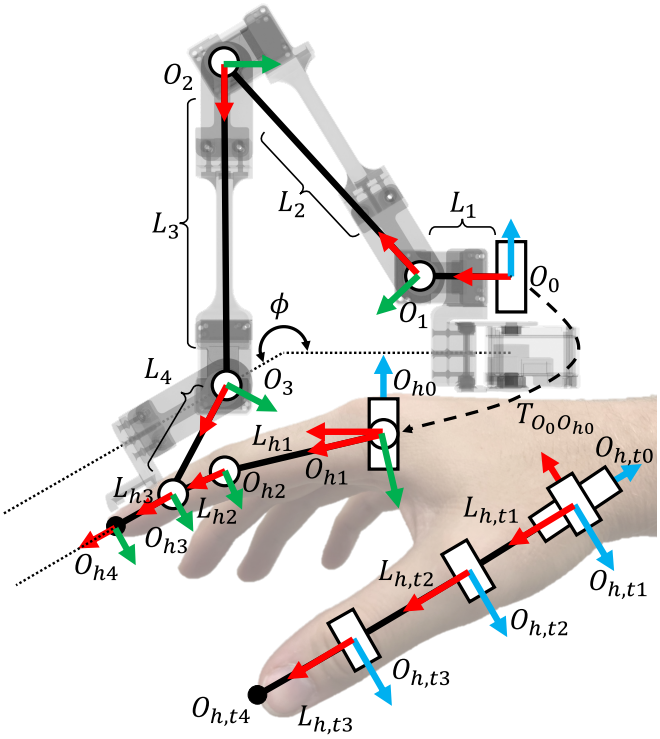

Fig. 2: Kinematic diagram of a user's hand when coupled with the APEX-Glove. Red, green, and blue arrows represent coordinate frame x, y, and z axes.

L_{h2}, and L_{h3} can be determined from L_h. Consequently, all necessary information is obtained to begin solving human finger IK. Notably, the thumb uses the same 4 DoF kinematic model, although its abductional axis protrudes through the back of the palm at approximately a 30° angle. Hence, a kinematic exoskeleton structure with four joints and an angled thumb is chosen.

2) Force Feedback: Producing kinesthetic 3D force feedback with an actuated manipulator was shown in [20], albeit without any regard for manipulator dynamics (friction, gravity, inertia), resulting in user exhaustion and opaque haptics. Thus, to create comfortable and transparent kinesthetic feedback, an analysis from robot dynamics is conducted. To begin, consider the general joint space dynamics of an n-link serial manipulator:

$$M(\boldsymbol{q})\ddot{\boldsymbol{q}} + C(\boldsymbol{q}, \dot{\boldsymbol{q}})\dot{\boldsymbol{q}} + g(\boldsymbol{q}) + \boldsymbol{\tau}_{fric} + \boldsymbol{\tau}_{ext} = \boldsymbol{\tau} \quad (1)$$

where $\boldsymbol{q}, \dot{\boldsymbol{q}}$, and $\ddot{\boldsymbol{q}}$ are all $\mathbb{R}^n$ vectors of *measured* robot joint positions, velocities, and accelerations. $M(\boldsymbol{q}) \in \mathbb{R}^{n\times n}$ is the mass matrix, $C(\boldsymbol{q}, \dot{\boldsymbol{q}}) \in \mathbb{R}^{n\times n}$ is a matrix of nonlinear Coriolis and centrifugal terms, $g(\boldsymbol{q}) \in \mathbb{R}^n$ is a configuration-dependent vector of gravitational torques, while $\boldsymbol{\tau}_{fric} \in \mathbb{R}^n$ and $\boldsymbol{\tau}_{ext} \in \mathbb{R}^n$ are the vectors of joint torques related to actuator friction and externally applied forces.

Given a perfectly parameterized model, commanding the robot joint torques using Equation (1) makes the system dynamically transparent (or "weightless") by exactly canceling out its bodily forces. Gravity and friction compensation are particularly useful for reducing user

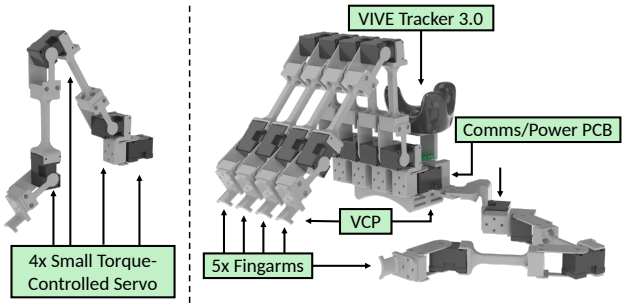

Fig. 3: Render of an individual Fingarm unit (left) and the assembled APEX-Glove with a VIVE Tracker attached for 6D pose measurement (right).

exertion within teleoperation [9], [27]. That said, *inertial compensation* is infeasible as the manipulator must comply with the unspecified motions of a mechanically-coupled human, obfuscating the acceleration trajectory needed to cancel out inertia. In practice, the sum of inertial, Coriolis, and gravity torques ($\boldsymbol{\tau}_{RNEA}$) is obtained using $\ddot{\boldsymbol{q}} = 0$ with the Recursive Newton-Euler Algorithm (RNEA) [27]. Beyond manipulator dynamic compensation, the serial robot must be able to apply a 3D force to the operator. This is done using the common external force relation:

$$\boldsymbol{\tau}_{ext} = J^T(\boldsymbol{q})\boldsymbol{F}_{ext} \tag{2}$$

where $J(\boldsymbol{q}) \in \mathbb{R}^{m \times n}$ is the geometric Jacobian matrix that maps differential changes in Cartesian and joint space, while $\boldsymbol{F}_{ext} \in \mathbb{R}^m$ is a desired wrench to render. Given that only 3D force feedback is desired, setting $m = 3$ ignores applying desired torques to the finger. After this, the joint is commanded with:

$$\boldsymbol{\tau}_{cmd} = \boldsymbol{\tau}_{RNEA} + \boldsymbol{\tau}_{fric} + \boldsymbol{\tau}_{ext} \tag{3}$$

Utilizing torques $\boldsymbol{\tau}_{cmd} \in \mathbb{R}^n$ will cause a serial robot to apply a desired force onto the operator's fingertip while compensating for robot dynamics to enhance transparency. This formulation can be applied to each exoskeletal structure to enable 3D force feedback on all fingers.

B. Hardware Implementation

1) System Design: The APEX-Glove, shown in Figure 3, is comprised of five 3D-printed, modular, inexpensive, kinesthetic finger-scale serial manipulators called *Fingarms*. A kinematic diagram of one *Fingarm* is shown in Figure 2 while its DH parameters are listed in Table I. Each Fingarm is an RRRR serial robot composed of Dynamixel XL330 servos at each joint. These servos are the most compact and lightweight current-controllable actuators commercially available. Only the low-geared variant (XL330-M077-T), with a reduction of 77:1, is used on the APEX-Glove. The higher-geared variant (XL330-M288-T) has $4\times$ the gearing, increasing torque by $4\times$ and apparent inertia by $16\times$. Despite the additional torque available with the higher geared variant, preliminary testing found that the additional inertia was too tiring to backdrive.

TABLE I: *Fingarm DH Parameters*

Link i	a_i $[mm]$	α_i $[rad]$	d_i $[mm]$	θ_i $[rad]$
1	L_1 = 35	$\pi/2$	0	q_1
2	L_2 = 109	0	0	q_2
3	L_3 = 102	0	0	q_3
4	L_4 = 55	0	0	q_4

All servos have absolute encoders for joint position sensing with a resolution of $0.088°$, which is $\sim 11\times$ better than the encoders used within [22]. Link lengths of the Fingarms are designed using the optimization procedure from [20] to ensure that a large adult male hand can fully open and close while wearing the device. Moreover, the large workspace of the APEX-Glove accommodates users with smaller-sized hands, too. For safety, the APEX-Glove utilizes sacrificial joint rotors that mechanically shear off of motor shafts in case of excessive external torques.

Beyond the Fingarms, the APEX-Glove also holds electronics for servo power distribution and communications. A tether is used to supply the actuators with 5V/4A power and USB-based control signals from a PC at a rate of 300 Hz. Exoskeleton 6D pose measurements are made by a VIVE Tracker 3.0 mounted on the back of the device. Nevertheless, the device is worn by coupling a user's hands to the Velcro Connection Points (VCP) on their fingertips and across their palm. This streamlines the donning/doffing process while enabling easy fit adjustments for improved comfort. Lastly, the device is designed to be inexpensive and easy to build; the material cost of a single unit, excluding the VIVE Tracker, sums to < 700 USD, as highlighted by the Bill of Materials shown in II. All mechanical parts are 3D-printed and fastened together with standard screws. Likewise, all onboard electronics are commercially available plug-and-play parts from ROBOTIS, thereby requiring minimal skills for device assembly. Moreover, the device is inherently modular, enabling Fingarms to be easily added/removed.

2) Data-Driven Actuator Modeling: While Dynamixel XL330 actuators possess unmatched size and cost, a major drawback of these servos is their plastic compound gearboxes. From [11], the relationship between input current commands and shaft output torque is nonlinear. Hence, the

TABLE II: *APEX-Glove Bill of Materials*

Part Name	Qty	Total Cost $[USD]$
Dynamixel XL330-M077-T	20	\$549.80
U2D2 USB-to-TTL Converter	1	\$36.92
Robotis 3P JST Exp. Board	1	\$6.79
1 kg PLA Filament Spool	1	\$19.99
Velcro Straps	1	\$7.95
25W Power Supply	1	\$16.99
Screw set	1	\$15.99
Bearing set	1	\$14.99
Total Price:		**\$669.42**

linear model from [20] which mapped desired torques to input current commands, had poor open-loop force control accuracy. To combat this, we fit a root model to [11]'s data:

$$\tau_{out} = a\sqrt{i_{cmd}} \tag{4}$$

here, $\tau_{out} \in \mathbb{R}$ represents the measured servo output torque while $i_{cmd} \in \mathbb{R}$ is the corresponding current command, and $a \in \mathbb{R}$ is a motor-specific parameter. Specifically, $a = 0.0045$ for XL330-M077-T, and $a = 0.0162$ for XL330-M288-T servos. This relationship has a Coefficient of Determination $R^2 > 0.98$, indicating a nearly perfect I/O fit, unlike [20]. This relationship is extended to negative current commands via ($\tau_{out} = sgn(i_{cmd})a\sqrt{|i_{cmd}|}$), before it is inverted as:

$$i_{cmd} = sgn(\tau_{out}) \left(\frac{\tau_{out}}{a}\right)^2 \tag{5}$$

Thus, Equation (5) enables low-cost XL330 servos to operate as open-loop torque-controlled actuators. Friction compensation is also needed at an actuator level to improve transparency further. To this end, input current vs. steady-state output speed data is collected for both actuator types. Figure 4 reveals curves showing static, kinetic, and viscous friction phenomena; these forces are modeled using a Coulomb-Viscous friction model:

$$\boldsymbol{\tau}_{fric} = \mu_v \dot{\boldsymbol{q}} + \mu_k sgn(\dot{\boldsymbol{q}}) \tag{6}$$

where $\mu_v \in \mathbb{R}$ and $\mu_k \in \mathbb{R}$ are the coefficients of viscous and kinetic friction. By varying these parameters, the friction model curve from Figure 4 can match the servo data, resulting in significantly less resistance when backdriving actuators. Static friction is overcome using high-frequency dithering on stationary joints, as done in [9].

C. Software Implementation

1) Architecture: The APEX-Glove's software architecture is designed to be modular, distributing computation over several purpose-built nodes powered by ROS2 [32]. Beyond interprocess communications, ROS2 enables easy integration with systems like Unity [33] that are commonly used in VR development and robotics simulation. Nonetheless, the software stack begins with a hardware management node establishing open-loop motor torque-control at 300 Hz, the maximum communication speed for a chain of 20 Dynamixel servos [11]. Despite this rate being slow for a torque-controlled system [27], it performs stably in practice. During every period, the hardware manager publishes exoskeleton joint positions $\boldsymbol{q}$ and finite-differenced velocities $\dot{\boldsymbol{q}}$ before commanding a new torque via Equation (3). Simultaneously, each finger's kinematics node determines corresponding human hand joint angles $\boldsymbol{q}_h$ based on $\boldsymbol{q}$. A dynamics node uses the RNEA algorithm from the rigid body dynamics library Pinocchio [34] to calculate $\boldsymbol{\tau}_{RNEA}$ and Fingarm Jacobians. Additionally, the gravity vector is rotated by the orientation of the VIVE Tracker to enable Fingarm gravity compensation regardless of device orientation. The dynamics node also computes $\boldsymbol{\tau}_{fric}$ and $\boldsymbol{\tau}_{ext}$, which are also sent to the hardware manager to actuate the exoskeleton's joints.

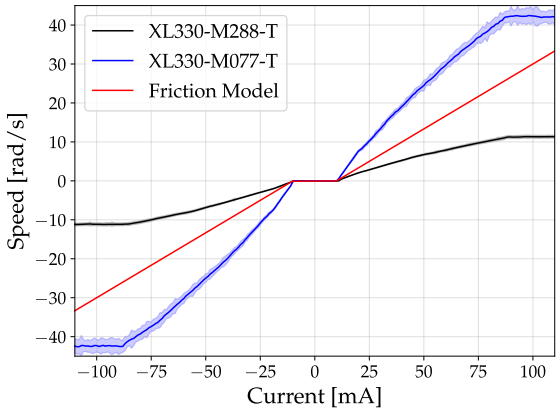

Fig. 4: Input current vs. joint speed for Dynamixel XL330 servos. Solid lines represent mean values while shaded regions show $\pm 1\sigma$. The red line displays an *untuned* Coulomb-Viscous friction model curve.

2) Haptic Force Generation: A key consideration in haptic systems is determining what triggers force display. Techniques like Virtual Contact Points or god objects are popular within simulations [27], whereas sensor-driven feedback is popular in telemanipulation [22]. Creating kinesthetic cues with god object rendering is a simple and effective technique that works across VR and real robot teleoperation. We use the strategy from [20] that superimposes two hand meshes in a virtual environment. One hand has colliders (the god object), while the other does not. Thus, when the pair of superimposed hands touches a virtual rigid body, the god hand is obstructed, creating a fingertip displacement. This is used to generate 3D force vectors via Hooke's Law: $\boldsymbol{F}_{haptic} = K_p \boldsymbol{x}$. Here, $K_p \in \mathbb{R}$ is a stiffness gain, whereas $\boldsymbol{x} \in \mathbb{R}^3$ is a position vector from the fingertip of the tracked hand to the god hand. Extending this formulation to teleoperation requires the god hand to mimic the real robot hand's joint pose, with displacements coming from real-world interactions. Communication latency creates small displacements if moving quickly, but thresholding $||\boldsymbol{x}||$ can alleviate this. A particular problem with the APEX-Glove system relates to actuator limitations. Due to the compact motor size and low servo gearing, $\boldsymbol{F}_{haptic}$ can saturate individual actuators, rendering haptic forces in the wrong directions. This is addressed by considering a *torque budget*, which is the remaining amount of torque that the actuators can apply towards rendering feedback before saturation:

$$\boldsymbol{\tau}_{budget} = K_{margin}\boldsymbol{\tau}_{sat} - abs\left(\boldsymbol{\tau}_{RNEA} - \boldsymbol{\tau}_{fric}\right) \tag{7}$$

Where $\boldsymbol{\tau}_{sat} \in \mathbb{R}^n$ is a vector of joint saturation torques, $K_{margin} \in [0, 1]$ is a safety margin, and $\boldsymbol{\tau}_{bud} \in \mathbb{R}^n$ is the torque budget. To counteract actuator saturation, a torque deficit $\boldsymbol{\tau}_{def} = abs(\boldsymbol{\tau}_{ext}) - \boldsymbol{\tau}_{bud}$ is used to determine a gain (K_{lim}) that scales down $\boldsymbol{F}_{haptic}$ to safe levels:

$$K_{lim} = min\left(\left[1.0, \boldsymbol{\tau}_{def} \oslash abs\left(J^T(\boldsymbol{q})\boldsymbol{F}_{haptic}\right)\right]\right) \tag{8}$$

where the $\oslash$ operator denotes vector element-wise division. With this, commanding $\boldsymbol{F}_{ext} = K_{lim}\boldsymbol{F}_{haptic}$

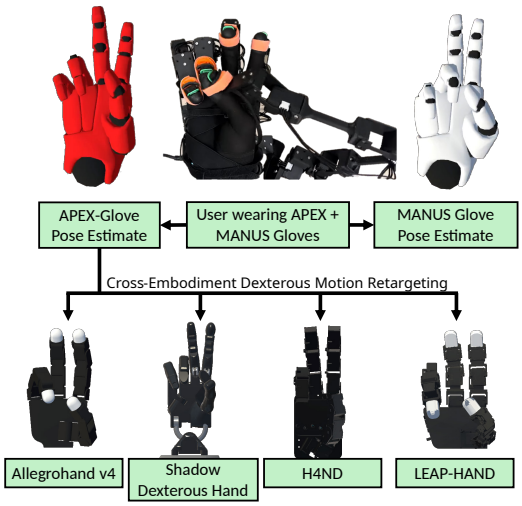

Fig. 5: Human hand wearing *both* the APEX-Glove and the MANUS Metagloves for mocap benchmarking (top) and retargeting to simulated robot hands (bottom).

guarantees that haptic forces are rendered in the correct direction by reducing magnitudes to respect actuator limits.

3) Hand Motion Retargeting: Translating human hand motions to multiple robotic hands is demonstrated in Unity using [35]. Joint angles obtained from the kinematics nodes are directly rendered onto a human hand mesh. Robot hand URDF models are scaled and superimposed over said meshes. Then, a numerical IK solver generates robot hand joint angles to track human fingertip motions.

III. Experimentation

This section summarizes the experimental campaign used to evaluate the APEX-Glove's motion capture, force-feedback, and dexterous hand control capabilities.

A. Motion Tracking Performance

Hand teleoperation requires *accurate motion capture* for human-robot retargeting. Central to this is a system's ability to infer human finger joint angles. To this end, the APEX-Glove's hand pose estimates are compared directly to the industrial-grade MANUS Quantum Metagloves [31], which provide 6 DoF magnetic-based tracking. As such, the Metagloves are considered a "ground-truth" for human joint angle measurements. The APEX-Glove is mounted on top of the Metagloves to enable comparable human motion capture data from both devices. Following calibration for each device, the wearer is instructed to mimic hand gestures from a prerecorded compilation video. Gestures range from Kapandji thumb opposability tests to pointing and making "peace signs". Renderings of each device's hand pose estimates are shown in Figure 5, with the APEX-Glove's tracking being shown in red while the Metagloves' are shown in white. Regardless of the user's capacity for recreating gestures, the simultaneity of recorded data can be used to determine APEX-Glove joint position inference errors.

B. Force-Feedback Verification

A simple experiment is conducted to verify the APEX-Glove's 3D force control capabilities. This experiment consists of fixing the device in space, placing the endpoint of a single Fingarm on a scale, and inputting force commands with gravity compensation until joint torque saturation occurs. The Fingarms are put into joint configurations with the smallest lever arms possible to maximize force output. This is repeated 10 times in all six directions ($\pm x, \pm y, \pm z$).

C. Haptic Robot Hand Teleoperation

The final experiment demonstrates APEX-Glove motion retargeting control of robotic hands in simulation and hardware (shown in Figure 1, right). Four simulated robot hands, each with corresponding superimposed god object hands, are fixed in space within Unity. Within the palm of each hand is a rigid capsule that a subject must grasp via the APEX-Glove. During a grasp, fingertip displacements generate force feedback on the operator's hands. This same concept is applied to real robot teleoperation, using real joint state feedback when grasping a rigid can.

IV. Results and Discussion

A. Experimental Results

A key performance indicator of the APEX-Glove's hand pose estimation system relates to its inferred joint positions compared to the Metagloves. Figure 5 displays corresponding index finger joint positions over a short period from one trial. Table III reports Root Mean Squared Error (RMSE) for each joint in the hand. Qualitatively, the APEX-Glove tracks the trajectory of the finger's planar joints, showing minimal error between the measured and ground truth signals for the MCP and PIP flexion joints. In contrast, the DIP flexion joint tracked the ground truth worse than others both qualitatively and quantitatively. While many joints presented some constant errors between the APEX-Glove and MANUS angles, DIP joint error is significantly affected by calibration; underestimates of human finger length result in the kinematic model "straightening out", dropping a term from the loop closure equation that solves for q_{h3}. Regardless, the average RMSE for all joints is $18.5°$, indicating the expected joint estimation error across the entire device. Despite this, such errors produce little *visual* effect on the output pose estimate, per Figure 5. The APEX-Glove's "peace sign" pose bears significant resemblance to the Metagloves' estimate. This same pose is then retargeted onto several simulated robot hands within Figure 5.

TABLE III: *Finger Motion Tracking RMSE [°]*

Joint	Index	Middle	Ring	Pinky	Thumb
MCP Abduct	5.84	6.92	10.96	13.85	4.79
MCP Flex	11.91	8.37	11.57	16.36	18.63
PIP Flex	20.25	16.91	19.04	23.69	36.33
DIP Flex	16.35	19.19	43.46	48.67	18.04

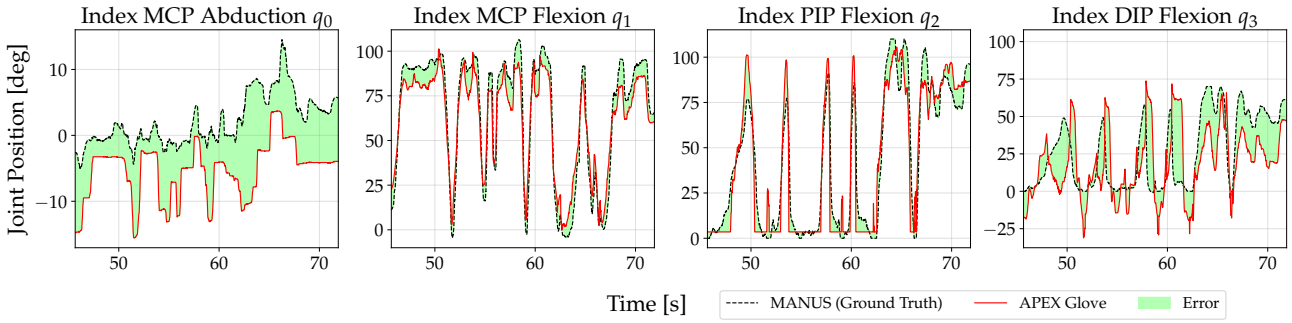

Fig. 6: Transient joint angle comparison between the APEX-Glove and "ground truth" measurements from MANUS [31].

Beyond motion capture performance, force control verification revealed that the system's average maximum open-loop output forces were 0.8 N, 0.7 N, and 1.4 N in the x, y, and z directions. Notably, the $\pm y$ directions possessed the lowest forces, as only a single actuator (q_0) pushes in that direction. $-z$ attained the highest force output once gravity compensation torques are overpowered by $\boldsymbol{\tau}_{ext}$, as a Fingarm could use its own weight to apply more force.

Moreover, the haptic teleoperation system successfully functioned for each of the robots tested, enabling users to feel what the robot was touching, per Figure 1. That being said, communication latency between the real robot hand and the APEX-Glove resulted in small erroneous force display when moving fingers rapidly. While thresholding does help mask such errors perceptively, proper control strategies for latency compensation are needed to improve the egocentric teleoperation experience further. Nevertheless, such latencies do not noticeably affect the system during simulated robot control in VR.

During early experimentation with the VR robot teleoperation simulator, we found that the 3D force feedback provided by the APEX-Glove was strong enough to immediately stop a user's fingers upon contacting an object, even when blindfolded. This was unexpected given the low magnitudes of force feedback provided by the exoskeleton. Moreover, 3D feedback allows users to feel both the hardness and weight of virtual objects simultaneously, making lateral manipulation in VR more immersive. Additionally, force feedback tended to improve physics simulator reliability during multifingered grasping, aligning with findings in [20].

B. Comparison to other Hand Feedback Devices

Lastly, we compare the APEX-Glove to several other prominent haptic exoskeletons from research and industry alike in Table IV. Despite having a relatively low maximum force output, **the APEX-Glove is the only wearable exoskeleton device capable of dynamical compensation and 3D bidirectional feedback**. HIRO III and ExoDex Adam show similar capabilities, but ultimately require external grounding, classifying them as non-exoskeletal systems. In contrast, actuated exoskeletons like Dexmo, DOGlove, and HEXOTRAC only display 1D feedback. The APEX-Glove weighs more than many of its counterparts at 870 g, although this is addressable by reducing the number of Fingarms. Additionally, the weight distribution of the Fingarms shifts the APEX-Glove's center of mass toward the operator's palm, thereby avoiding the torsional forearm discomfort that affected [20]. Despite this, the device is still bulky (in terms of size) compared to most other exoskeletons, primarily due to actuator dimensions. With thinner actuators, ergonomics (and overall haptic strength) can be improved significantly.

V. Conclusion

This work presented the APEX-Glove, the world's first wearable kinesthetic hand exoskeleton. By using the latest advancements in small, commercial-off-the-shelf, current-controlled actuators, the APEX-Glove produces up to 1.4 N of arbitrarily directed 3D force feedback on each of a user's fingertips independently. Moreover, kinematic modeling of human finger joints enable the proposed device to estimate a wearer's finger joint positions in real-time. Compared to a ground truth, such estimates have an average joint RMSE of $18.5°$. Furthermore, the APEX-Glove is demonstrated in simulated and real robotic hand teleoperation with 3D force feedback, demonstrating that novel haptic interfaces can bridge current limitations in teleoperated robot hand force awareness. Nonetheless, improvement is still possible; sensorizing the human fingertip connection points can enable admittance control for increased transparency. More robust knuckle pose estimation is possible with finger pose following calibration. Better inertial compensation can enable stronger actuators (XL330-M288-T) to be used to greatly improve force feedback performance. Additionally, VR manipulation and medical hand rehabilitation are targeted future applications. Lastly, we open-source the APEX-Glove's inexpensive hardware, software, and assembly tutorials to disseminate accurate motion retargeting and 3D force feedback to the community.

References

[1] J. Vaz, N. Kosanovic and P. Oh, "ART: Avatar Robotics Telepresence—the future of humanoid material handling loco-manipulation," in *Intel Serv Robotics*, Dec. 2023. doi: 10.1007/s11370-023-00499-x [Online].

[2] Y. Park, J. S. Bhatia, L. Ankile, and P. Agrawal, "DexHub and DART: Towards Internet Scale Robot Data Collection," in *CoRL-X-Embodiment 2024 Workshop*, Online, Nov. 2024.

[3] ALOHA 2 Team, "ALOHA 2: An Enhanced Low-Cost Hardware for Bimanual Teleoperation," *arXiv*, preprint arXiv:2405.02292 [cs.RO], Feb. 2024.

TABLE IV: *Comparison of Kinesthetic Force Feedback Devices*

Device Name	Mechanism	Exoskeleton?	Actuators/Finger	Feedback Dim.	Dyna. Comp.?	Max Force $[N]$	Weight $[g]$	Cost $[USD]$
APEX-Glove	Actuated Exoskel.	✓	**4**	3D	✓	1.4	870	< 700
HIRO III [28]	Robot Hand	✗	3	3D	✓	3.6	780	Unknown
ExoDex Adam [29]	Robot Hand	✗	3	3D	✓	10	2500	Unknown
Dexmo [18]	4-bar Linkage	✓	1	1D	✗	~ 16	300	12000
DOGlove [22]	4-bar Linkage	✓	1	1D	✗	Unknown	550	600
HEXOTRAC [23]	4-bar Linkage	✓	1	1D	✗	4.8	Unknown	Unknown
SenseGlove [24]	Tendon	✓	1	1D Unidir.	✗	20	320	7000
HaptX G1 [25]	Tendon	✓	1	1D Unidir.	✗	35.6	570	4500

[4] A. O'Neill *et al.*, "Open X-Embodiment: Robotic Learning Datasets and RT-X Models : Open X-Embodiment Collaboration,"*2024 IEEE International Conference on Robotics and Automation (ICRA)*, Yokohama, Japan, 2024, pp. 6892-6903, doi: 10.1109/ICRA57147.2024.10611477.

[5] C. Chen, Z. Yu, H. Choi, M. Cutkosky and J. Bohg, "DexForce: Extracting Force-Informed Actions From Kinesthetic Demonstrations for Dexterous Manipulation," in *IEEE Robotics and Automation Letters*, vol. 10, no. 6, pp. 6416-6423, June 2025, doi: 10.1109/LRA.2025.3568318.

[6] M. Xu, *et al.*, "DexUMI: Using Human Hand as the Universal Manipulation Interface for Dexterous Manipulation", arXiv:2505.21864 [cs.RO], May. 2025.

[7] H.-S. Fang *et al.*, "DEXOP: A Device for Robotic Transfer of Dexterous Human Manipulation," in *Proc. Workshop on Human-Robot Contact and Manipulation (HRCM), Robotics: Science and Systems (RSS)*, Los Angeles, CA, USA, Jun. 2025.

[8] D. Wei and H. Xu, "A Wearable Robotic Hand for Hand-over-Hand Imitation Learning," *2024 IEEE International Conference on Robotics and Automation (ICRA)*, Yokohama, Japan, 2024, pp. 18113-18119, doi: 10.1109/ICRA57147.2024.10610516.

[9] J. J. Liu, *et al.*, "FACTR: Force-Attending Curriculum Training for Contact-Rich Policy Learning," *arXiv*, preprint arXiv:2502.17432.

[10] Y. Dong, X. Liu, J. Wan and Z. Deng, "GEX: Democratizing Dexterity with Fully-Actuated Dexterous Hand and Exoskeleton Glove", *arXiv*, preprint arXiv:2506.04982 [cs.RO], Jun. 2025.

[11] N. Kosanovic and J. C. Vaz, "Humans and Robots, Hand-in-Hand: Using Bilateral Telepresence to Turn Robotic Hands into Wearable Haptic Exoskeletons," *2025 22nd International Conference on Ubiquitous Robots (UR)*, College Station, TX, USA, 2025, pp. 67-74, doi: 10.1109/UR65550.2025.11078031.

[12] M. Kobayashi, T. Buamanee and T. Kobayashi, "ALPHA-α and Bi-ACT Are All You Need: Importance of Position and Force Information/ Control for Imitation Learning of Unimanual and Bimanual Robotic Manipulation With Low-Cost System," in *IEEE Access*, vol. 13, pp. 29886-29899, 2025, doi: 10.1109/ACCESS.2025.3541200.

[13] K. Li *et al.*, "Haptic-ACT: Bridging Human Intuition with Compliant Robotic Manipulation via Immersive VR," *arXiv*, preprint arXiv:2409.11925 [cs.RO], Mar. 2025.

[14] T. L. Gibo, A. J. Bastian and A. M. Okamura, "Grip Force Control during Virtual Object Interaction: Effect of Force Feedback, Accuracy Demands, and Training," in *IEEE Transactions on Haptics*, vol. 7, no. 1, pp. 37-47, Jan.-March 2014, doi: 10.1109/TOH.2013.60.

[15] J. A. Fishel *et al.*, "Tactile Telerobots for Dull, Dirty, Dangerous, and Inaccessible Tasks," *2020 IEEE International Conference on Robotics and Automation (ICRA)*, Paris, France, 2020, pp. 11305-11310, doi: 10.1109/ICRA40945.2020.9196888.

[16] G. Santamato *et al.*, "Anywhere Is Possible: An Avatar Platform for Social Telepresence With Full Perception of Physical Interaction," in *IEEE Access*, vol. 12, pp. 70926-70945, 2024, doi: 10.1109/ACCESS.2024.3402090.

[17] Z-H. Yin, *et al.*, "DexterityGen: Foundation Controller for Unprecedented Dexterity", *arXiv*, preprent arXiv:2502.04307 [cs.RO], Feb. 2025.

[18] K. Krieger *et al.*, "Adaptive Kinematic Modeling for Improved Hand Posture Estimates Using a Haptic Glove," *arXiv* preprint arXiv:2411.06575 [cs.RO], Nov. 2024.

[19] E. Sung, S. You, S. Moon, J. Kim and J. Park, "SNU-Avatar Haptic Glove: Novel Modularized Haptic Glove via Trigonometric Series Elastic Actuators", *2024 IEEE/RSJ International Conference on Intelligent Robots and Systems (IROS)*, Abu Dhabi, United Arab Emirates, 2024, pp. 3573-3580, doi: 10.1109/IROS58592.2024.10802590.

[20] N. Kosanovic and J. C. Vaz, "Wearing a Robotic Hand to Feel 3D Force Feedback: Analysis and Virtual Reality Application of the Hand-in-Hand System," *2025 IEEE/RSJ International Conference on Intelligent Robots and Systems (IROS)*, Hangzhou, China, 2025, pp. 13955-13962, doi: 10.1109/IROS60139.2025.11246130.

[21] M. Aiple and A. Schiele, "Pushing the limits of the CyberGrasp for haptic rendering," *2013 IEEE International Conference on Robotics and Automation*, Karlsruhe, Germany, 2013, pp. 3541-3546, doi: 10.1109/ICRA.2013.6631073.

[22] H. Zhang, S. Hu, Z. Yuan and H. Xu, "DOGlove: Dexterous Manipulation with a Low-Cost Open-Source Haptic Force Feedback Glove", *arXiv*, preprint arXiv:2502.07730 [cs.RO], Feb. 2025.

[23] I. Sarakoglou, A. Brygo, D. Mazzanti, N. G. Hernandez, D. G. Caldwell and N. G. Tsagarakis, "HEXOTRAC: A highly under-actuated hand exoskeleton for finger tracking and force feedback," *2016 IEEE/RSJ International Conference on Intelligent Robots and Systems (IROS)*, Daejeon, Korea (South), 2016, pp. 1033-1040, doi: 10.1109/IROS.2016.7759176.

[24] "*SenseGlove Nova 2*." https://www.senseglove.com/product/nova-2/.

[25] "*HaptX G1*." haptx.com. https://support.haptx.com/specs-features/.

[26] E. Saerens *et al.*, "Scaling laws for parallel motor-gearbox arrangements," *2020 IEEE/RSJ International Conference on Intelligent Robots and Systems (IROS)*, Las Vegas, NV, USA, 2020, pp. 6339-6346, doi: 10.1109/IROS45743.2020.9341309.

[27] B. Sciliano and O. Khatib, *Springer Handbook of Robotics*, 1st ed., Heidelberg, Springer Berlin, 2008, pp. 719-739. [Online]. Available: https://doi.org/10.1007/978-3-540-30301-5.

[28] T. Mouri, H. Kawasaki and S. Ueki, "Teleoperated humanoid hand robot using force feedback," *2015 IEEE/SICE International Symposium on System Integration (SII)*, Nagoya, Japan, 2015, pp. 942-947, doi: 10.1109/SII.2015.7405139.

[29] N. Y. Lii *et al.*, "Exodex Adam—A Reconfigurable Dexterous Haptic User Interface for the Whole Hand," in *Haptics, Frontiers in Robotics and AI*, vol. 8, Article 716598, Mar. 2022. doi: 10.3389/frobt.2021.716598.

[30] Y. Su, G. Li, Y. Deng, I. Sarakoglou, N. G. Tsagarakis and J. Chen, "The Joint-Space Reconstruction of Human Fingers by using a Highly Under-Actuated Exoskeleton," *2024 IEEE International Conference on Robotics and Automation (ICRA)*, Yokohama, Japan, 2024, pp. 9645-9651, doi: 10.1109/ICRA57147.2024.10610872.

[31] MANUS Technology Group, "Quantum Metagloves," *MANUS Meta*.

[32] Macenski, T. Foote, B. Gerkey, C. Lalancette, W. Woodall, "Robot Operating System 2: Design, architecture, and uses in the wild," in *Sci. Rob.*, vol. 7, May 2022.

[33] "Unity-Robotics-Hub," GitHub repository, 2022. [Online]. Available: https://github.com/Unity-Technologies/Unity-Robotics-Hub.

[34] J. Carpentier *et al.*, "The Pinocchio C++ library: A fast and flexible implementation of rigid body dynamics algorithms and their analytical derivatives," *2019 IEEE/SICE International Symposium on System Integration (SII)*, Paris, France, 2019, pp. 614-619, doi: 10.1109/SII.2019.8700380.

[35] N. Kosanovic and J. C. Vaz, "A Virtual Reality Framework for Safe Global Bimanual Telepresence," *2025 IEEE 21st International Conference on Automation Science and Engineering (CASE)*, Los Angeles, CA, USA, 2025, pp. 3412-3419, doi: 10.1109/CASE58245.2025.11164157.